Title
Restricting 32–128 km horizontal scales hardly affects the MJO in the Superparameterized Community Atmosphere Model v.3.0 but the number of cloud-resolving grid columns constrains vertical mixing

Journal
Journal of Advances in Modeling Earth Systems, 6(3)

ISSN
1942-2466

Authors
Pritchard, Michael S
Bretherton, Christopher S
DeMott, Charlotte A

Publication Date
2014-09-01

DOI
10.1002/2014ms000340

AGU PUBLICATIONS

Journal of Advances in Modeling Earth Systems

RESEARCH ARTICLE

10.1002/2014MS000340

Key Points:

- Physics of MMF MJO are insensitive to near elimination of meso-beta-scale
- The efficiency of deep convective mixing in MMFs is limited by CRM extent
- 4x speedup of superparameterized models possible for MJO analysis

Correspondence to:
M. S. Pritchard,
mspritch@uci.edu

Citation:
Pritchard, M. S., C. S. Bretherton, and C. A. DeMott (2014), Restricting 32–128 km horizontal scales hardly affects the MJO in the Superparameterized Community Atmosphere Model v.3.0 but the number of cloud-resolving grid columns constrains vertical mixing, *J. Adv. Model. Earth Syst.*, *6*, 723–739, doi:10.1002/2014MS000340.

Received 27 APR 2014
Accepted 30 JUN 2014
Accepted article online 9 JUL 2014
Published online 5 AUG 2014

Restricting 32–128 km horizontal scales hardly affects the MJO in the Superparameterized Community Atmosphere Model v.3.0 but the number of cloud-resolving grid columns constrains vertical mixing

Michael S. Pritchard[1], Christopher S. Bretherton[2], and Charlotte A. DeMott[3]

[1]Department of Earth System Sciences, University of California, Irvine, California, USA, [2]Department of Atmospheric Sciences, University of Washington, Seattle, Washington, USA, [3]Department of Atmospheric Science, Colorado State University, Fort Collins, Colorado, USA

Abstract The effects of artificially restricting the 32–128 km horizontal scale regime on MJO dynamics in the Superparameterized Community Atmosphere Model v.3.0 have been explored through reducing the extent of its embedded cloud resolving model (CRM) arrays. Two and four-fold reductions in CRM extent (from 128 to 64 km and 32 km) produce statistical composite MJO signatures with spatial scale, zonal phase speed, and intrinsic wind-convection anomaly structure that are all remarkably similar to the standard SPCAM's MJO. This suggests that the physics of mesoscale convective organization on 32–128 km scales are not critical to MJO dynamics in SPCAM and that reducing CRM extent may be a viable strategy for 400% more computationally efficient analysis of superparameterized MJO dynamics. However several unexpected basic state responses caution that extreme CRM domain reduction can lead to systematic mean state issues in superparameterized models. We hypothesize that an artificial limit on the efficiency of vertical updraft mixing is set by the number of grid columns available for compensating subsidence in the embedded CRM arrays. This can lead to reduced moisture ventilation supporting too much liquid cloud and thus an overly strong cloud shortwave radiative forcing, particularly in regions of deep convection.

1. Introduction

The physics of the Madden-Julian Oscillation [*Madden and Julian*, 1972] are still in debate over 40 years since its discovery, and there is no consensus for a simple dynamical paradigm to explain it. Progress on this front is critical to understand its interaction with tropical climate dynamics and climate change.

Modern MJO theories such as the multiscale and "skeleton" models of *Biello and Majda* [2005]; *Khouider and Majda* [2006]; *Majda and Stechmann* [2009] and the "moisture mode" ideas of *Raymond and Fuchs* [2009] and *Sobel and Maloney* [2012, 2013]—while in agreement about a fundamental role for moisture variations in the tropics—tend to emphasize different dynamical processes to help explain MJO physics. Some incarnations of the multiscale paradigm emphasize upscale momentum transport by the physics of mesoscale convective organization, and the importance of second or third-baroclinic heating modes due to the convective lifecycle. In contrast, some incarnations of the moisture-mode paradigm emphasize the importance of horizontal moisture advection, and column thermodynamic properties such as the gross moist stability, cloud-radiative and surface flux thermodynamic feedbacks. To the extent that both paradigms can succeed in capturing key observed MJO relationships in a minimal mathematical model, it can be difficult to find consensus for selecting between them.

In this context, it is especially important to explore the behavior of global models that make minimal assumptions about how deep convection behaves. If such a model can capture convincingly realistic MJO signals, it can be applied to explicitly test the criticality of processes emphasized by competing dynamical paradigms, in a relatively agnostic sense.

Global cloud resolving models (GCRMs) are an obviously attractive candidate. For instance, the Nonhydrostatic ICosohedral Atmospheric Model (NICAM)—which explicitly resolves deep convection globally, by covering the entire planet in convection-resolving (1–10 km) horizontal resolution, and which exhibits some

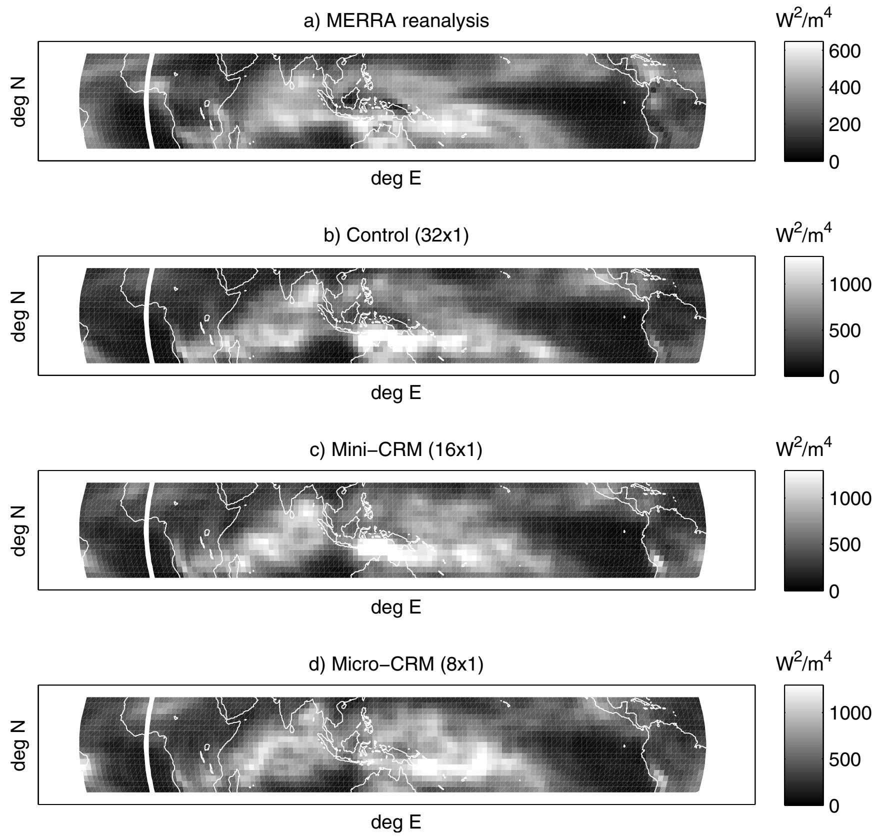

Figure 1. (a) Observed, (b) control, and (c and d) test simulated 20–100 day bandpass filtered variance of daily outgoing longwave radiation anomalies during NDJF. Note the color scale in Figure 1a is half the amplitude as the other plots.

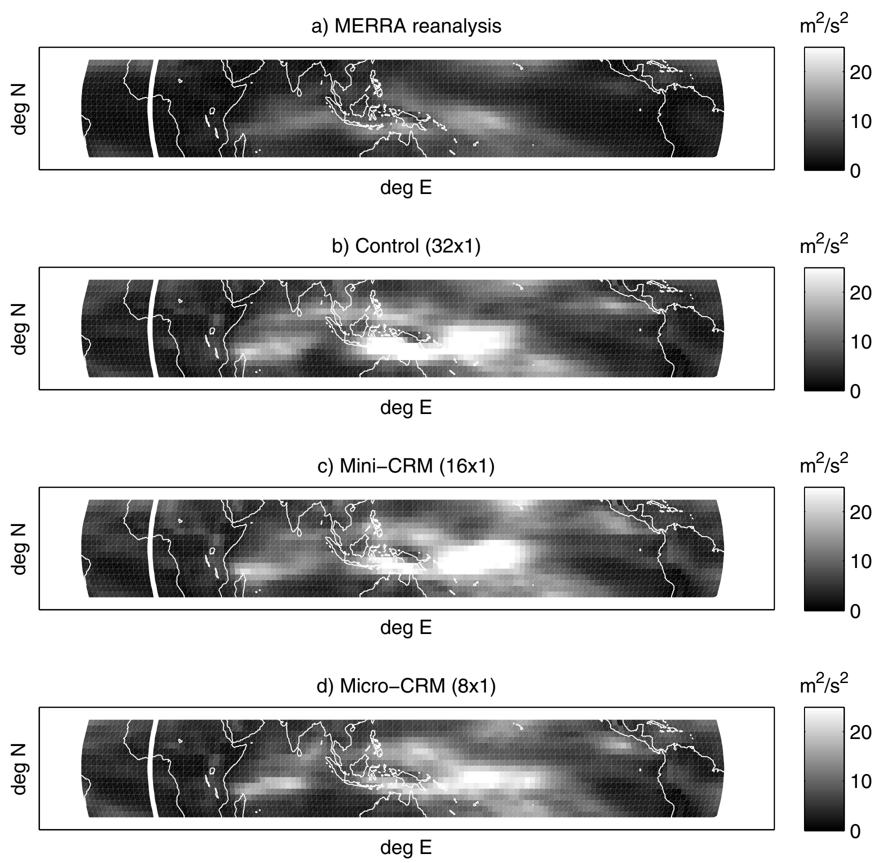

Figure 2. As in Figure 1 but for 850 hPa zonal wind anomalies. Note the color scale is consistent for all plots.

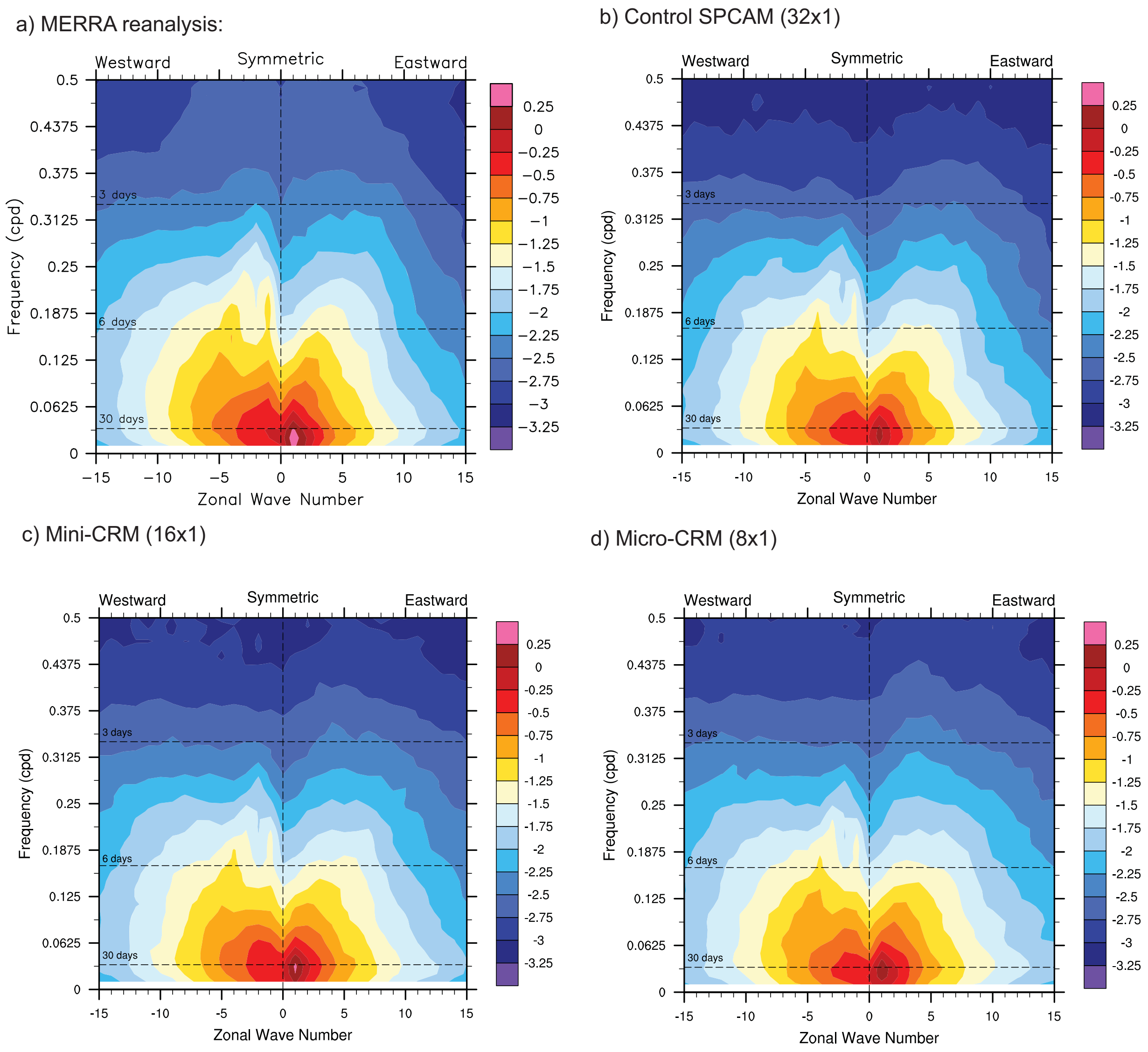

Figure 3. Wavenumber-frequency raw spectral power of equatorially symmetric (15S-15N) daily 850 hPa zonal wind anomalies during all seasons for (a) observations and (b)–(d) all SPCAM simulations.

success at hindcasting observed MJO activity [*Miyakawa et al*., 2014]. But GCRMs are currently impractical for detailed iterative MJO hypothesis testing as they tax available hardware and require time-intensive data processing to analyze.

A less computationally daunting modeling approach is superparameterization, which reduces the computational expense of explicitly resolving deep convection by confining it to idealized two-dimensional cloud resolving model subdomains embedded inside a coarse-resolution hydrostatic GCM [*Grabowski*, 2001; *Randall et al*., 2003]. This "heterogeneously multiscale" approach can produce realistic MJO dynamics making minimal assumptions about deep convection and its coupling to planetary scale dynamics. For example, the uncoupled Superparameterized Community Atmosphere Model (SPCAM) v3.0 [*Khairoutdinov et al*., 2005] produces a boreal winter MJO in which both dynamic and thermodynamic height-time anomaly composites validate well against reanalysis observations [*Khairoutdinov et al*., 2008; *Benedict and Randall*, 2009].

We have recently explored the question of whether the realistic MJO in SPCAM *depends* on explicitly resolving horizontal scales in the 32–128 km regime. The artificial scale separation of superparameterization

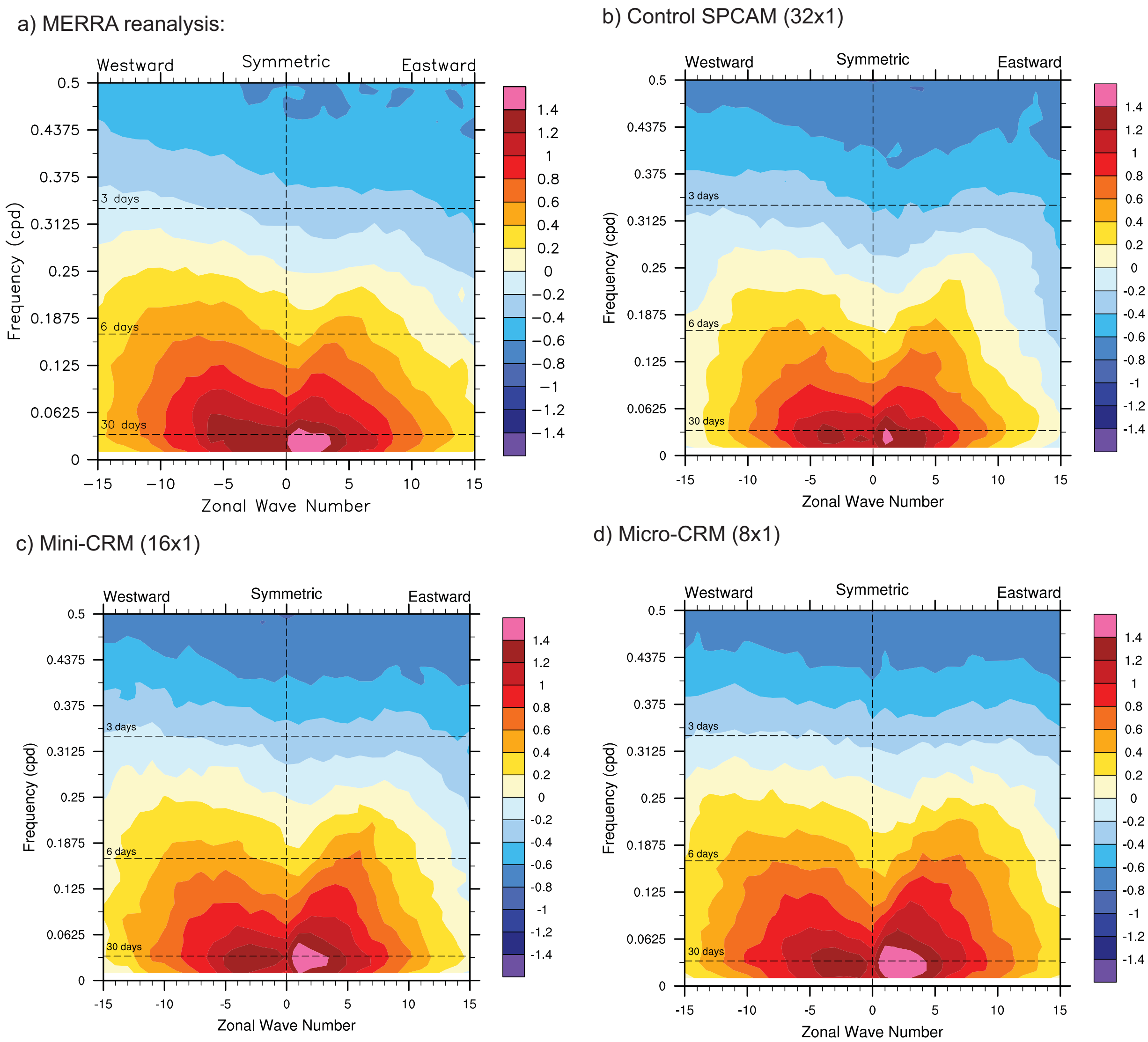

Figure 4. As in Figure 3 but for the spectral power of outgoing long-wave radiation anomalies.

provides a convenient way to test this by *restricting this scale regime*. *Pritchard and Bretherton* [2014, Figure 1] showed a striking insensitivity of the superparameterized MJO to eliminating these scales through a reduction from 128 to 32 km CRM domain extent.

The purpose of this paper is to explore in more detail the consequences of radically reducing the extent of SPCAM's embedded CRM arrays – both for the MJO and for the simulated mean state. To better understand systematic responses to reduced CRM domains we sample three configurations—the standard 128 km extent, an intermediary 64 km case and the previously tested 32 km case—the latter being a domain size so small (only 8 CRM columns per array) that it can be expected to severely restrict the degree to which multiply interacting cloud types and thus mesoscale convective organization can occur, as discussed by *Pritchard and Bretherton* [2014]. We call these reconfigurations "Mini-CRM" (64 km extent) and "Micro-CRM" (32 km extent). More details about the modeling setup are provided in section 2.

A practical objective of exploring reduced CRM domain extents is to see if the computational efficiency of superparameterization can be enhanced for more efficient numerical analysis of MJO dynamics or even global change without compromising simulation performance. Reduced CRM extent could be a strategy for faster simulations—for instance, Micro-CRM runs 4 times faster than the standard model. The sensitivities to

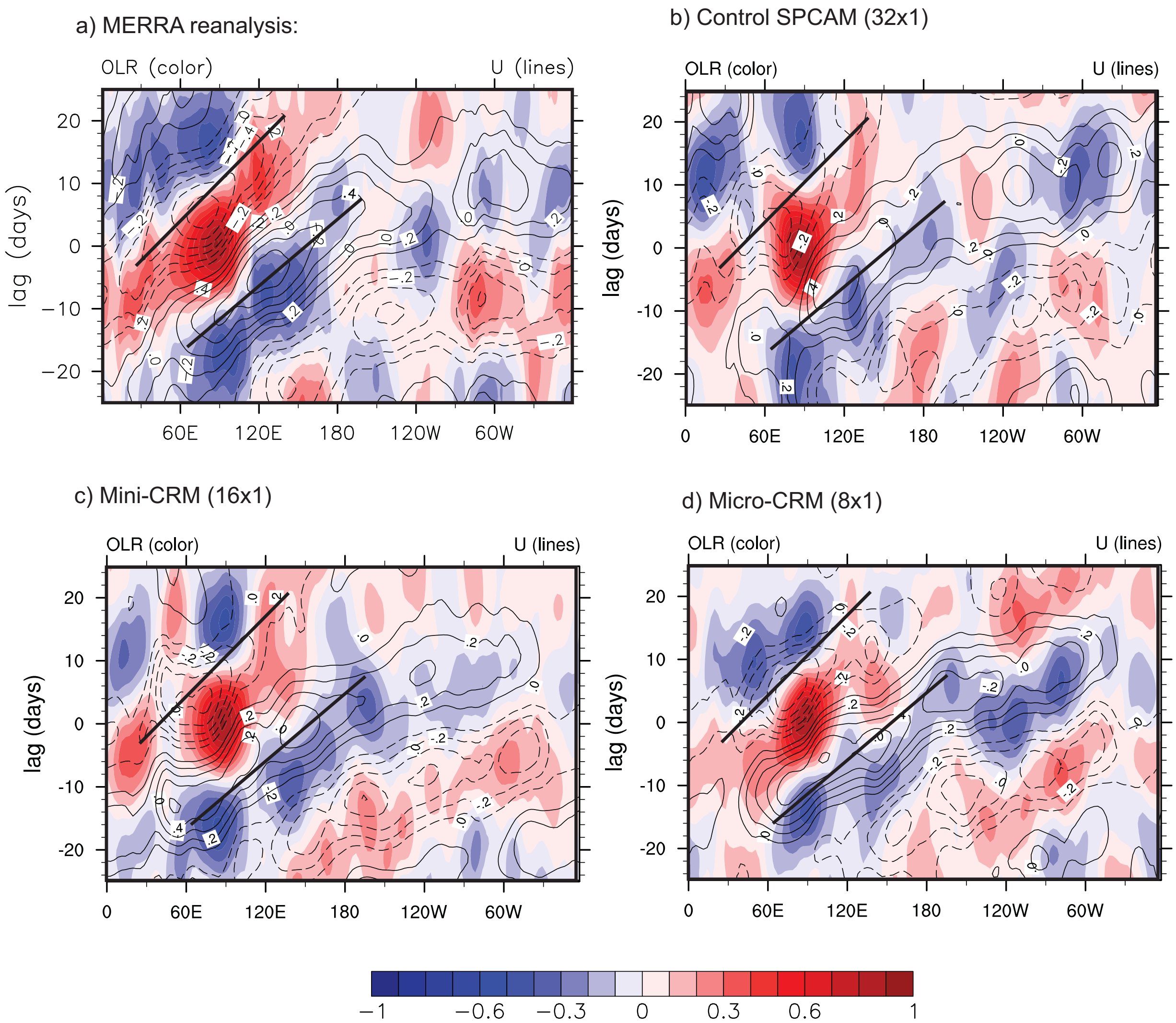

Figure 5. Longitude and time lag-correlation coefficients for (colors) outgoing longwave radiation versus (contours) 850 hPa zonal anomalies in 15S–15N regressed against a 20–100 day filtered OLR anomaly time series at 80°E. Results are for boreal winter only, comparing Figure 4a the observed composite MJO against (Figures 4b and 4d) all SPCAM simulations. The observed MJO zonal phase speed is superimposed in all plots (black lines).

domain reduction are also important to document given that the current 128 km CRM extent in SPCAM can be viewed as somewhat arbitrary.

Micro-CRM is not a new idea. An 8 column, 32 km CRM configuration was previously explored by *Khairoutdinov et al*. [2005] who reported that it interestingly did not significantly alter several aspects of the mean climate in SPCAM3.0. In short-duration simulations, episodes of simulated intraseasonal variability also seemed qualitatively robust to using Micro-CRM (D. Randall, personal communication). Statistical robustness of the intraseasonal portion of the equatorial OLR spectrum was recently confirmed by *Pritchard and Bretherton* [2014]. The impact of Mini-CRM (16 columns) has not previously been reported in the literature. In general, the role the mesoscale plays in producing favorable emergent MJO and mean state behavior in superparameterized simulations has not been explored in detail.

The rest of this paper proceeds as follows. Section 2 describes the model and experiment design. The results in section 3.1 show that SPCAM's high quality boreal winter MJO is mostly robust to a near-elimination of the 32 to 128 km horizontal scale regime. The mean state is analyzed in section 3.2, uncovering a surprising sensitivity of shortwave cloud forcing and liquid clouds. Discussion and a hypothesis for the latter response is in section 4 and conclusions are summarized in section 5.

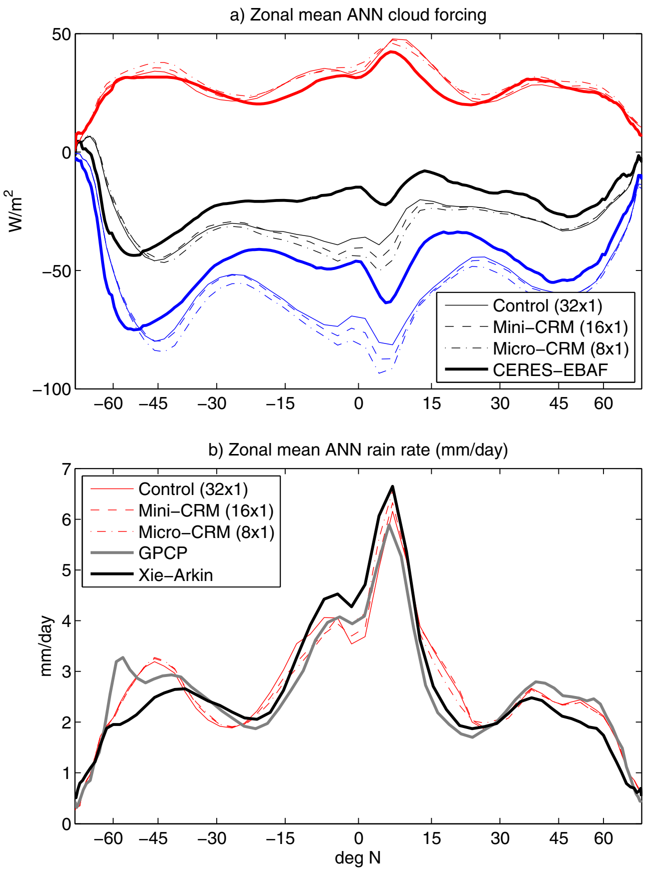

Figure 6. (a) Annual zonal mean (black) net cloud radiative forcing and its (red) longwave versus (blue) shortwave components in (thick lines) observations versus (solid) standard SPCAM and (dashed, dotted) using Mini, Micro-CRM. (b) (Black, gray) observed versus (red) simulated annual and zonal mean rainfall rate.

2. Methodology

2.1. The Model

The baseline version of SPCAM3.0 used in this study is almost identical to that analyzed previously by *Khairoutdinov et al.* [2005, 2008]; *Benedict and Randall* [2009]; and *Thayer-Calder and Randall* [2009]. Readers are referred to *Pritchard and Bretherton* [2014] for further background. For reproducibility, the version of code used in this study is archived (https://svn.sdsc.edu/repo/cmmap/cam3_sp/branches/pritchard (rev. 304)) at the Center for Multiscale Modeling of Atmospheric Processes.

2.2. The Experiments

Three SPCAM simulations are performed as follows. The first is a 10 year control run using SPCAM's standard superparameterization configuration of embedding rather "large" (128 km long, 32 column) cloud resolving arrays that encompass most of the mesoscale. The CRMs are oriented north-south. Two 10 year test runs are then done using the "Mini-CRM" (64 km long, 16 column) and "Micro-CRM" (32 km long, 8 column) approaches. They are forced identically to the control run. All simulations are initialized in September 1980 and terminated in December 1990. The first 4 months are discarded as spinup. For reference, simulated MJO structures are compared to a 20 year climatological signal from the MERRA reanalysis (1989–2009) interpolated horizontally to SPCAM's horizontal resolution. Each decadal simulation provides a sufficiently long record to analyze the basic character of the simulated boreal winter MJO statistically, as follows.

3. Results

We begin by applying standard MJO diagnostic techniques [*Kim et al*., 2009]. Intraseasonal anomalies of outgoing longwave radiation, lower and upper-level winds are calculated relative to a smoothed mean annual cycle for each run. From these we compute a comprehensive suite of MJO diagnostics, building up from 20 to 100 day bandpass filtered anomaly variance analysis, to wave number-frequency spectral decomposition across all intraseasonal time scales, and ultimately to lag-correlation analysis. The results give a holistic view of the simulated MJO from several vantage points, which will show an interesting *insensitivity* of the superparameterized MJO to shrinking the extent of its embedded CRM arrays by factors of 2 and 4. Trivariate empirical orthogonal function decomposition using the approach of *Wheeler and Hendon* [2004] confirms this finding, but is not shown for brevity.

3.1. MJO Response

Figure 1 examines the effect of reduced CRM extent on the horizontal structure of 20–100 day filtered variance in outgoing longwave radiation. Both versions of SPCAM have too much intraseasonal OLR variance, by

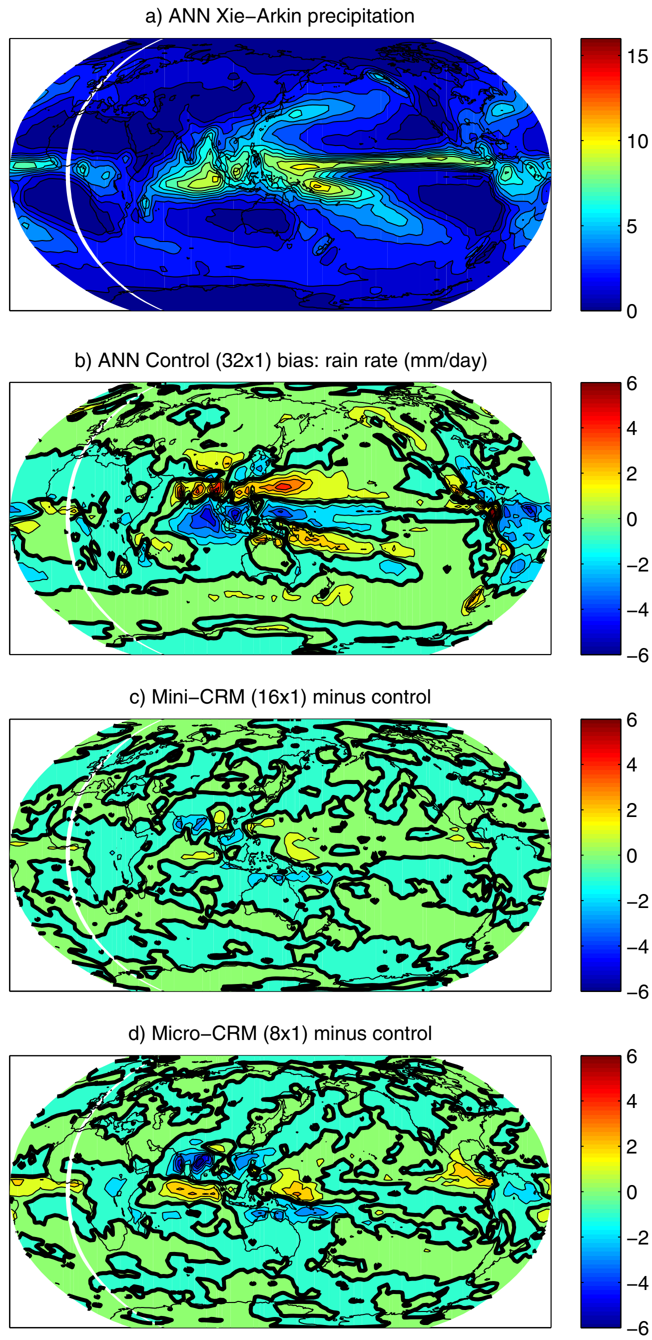

Figure 7. Annual mean precipitation (a) from the Xie-Arkin data product and versus (b) the bias in the control version of SPCAM, and (c and d) the additional change that results from reducing the CRM extent, relative to the control. The contour interval is 1 mm/d in all subplots.

almost a factor of two (note distinct color scales in Figure 1a versus other plots). This is a well known bias in the baseline uncoupled SPCAM3.0—it produces a realistic MJO signal, but with greatly exaggerated amplitude [*Benedict and Randall*, 2009]. There are some regional differences, but overall reducing the CRM extent does not strongly impact the overall magnitude and spatial pattern of intraseasonal fluctuations in both winds and convection—which resemble the standard model in both the Mini and Micro-CRM configurations.

The 850 hPa zonal wind intraseasonal variance in Figure 2 is also fairly insensitive to the CRM extent. Again, all the simulations overestimate the overall variance compared to observations, but to a lesser extent than for OLR.

Tropical modes of low-level wind variability appear strikingly insensitive to reduced CRM extent from the holistic diagnostic perspective of wave number-frequency analysis. Figure 3 reveals virtually indistinguishable wind spectra in all SPCAM simulation configurations. Neither the dominant MJO feature (eastward zonal wave number 1 and time scales greater than 30 days) nor the background red noise component of tropical zonal wind variability is strongly affected from this perspective.

Wave number-frequency analysis of outgoing longwave radiation in Figure 4 confirms the general insensitivity of the MJO spectral feature to CRM extent. That is, the raw OLR spectral feature in the MJO scale regime resembles the standard model's signal, albeit riding atop a higher amplitude red noise background (which is somewhat of an improvement) but with qualitatively comparable east-west power ratio. However analysis of the corresponding OLR signal-to-noise spectra (not shown) indicates there is a somewhat unfavorable blurring of the distinct separation between the Moist Kelvin Wave (MKW) and MJO modes, especially in the extreme case of Micro-CRM.

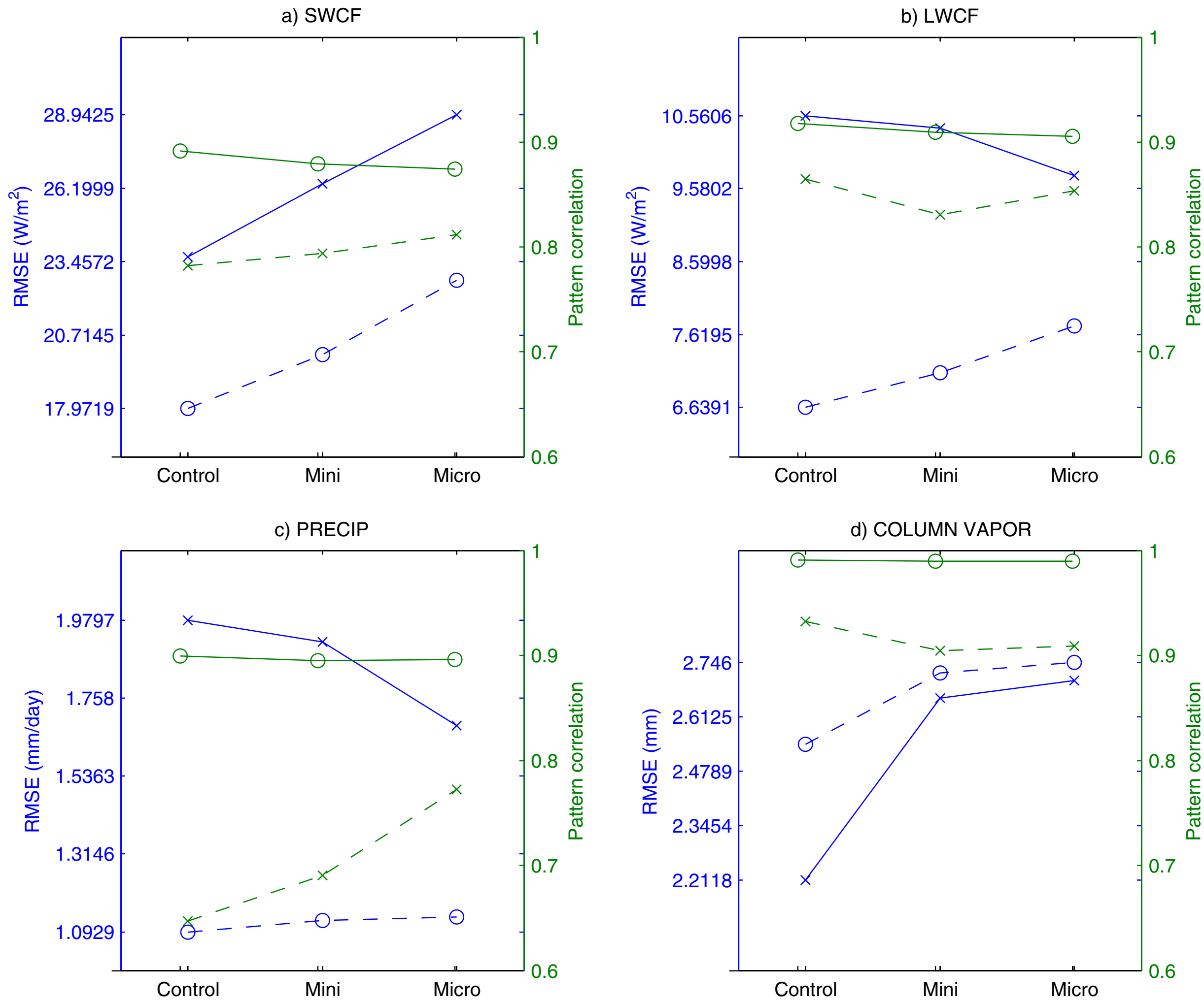

Figure 8. Annual climatological mean model bias measured as (blue) area-weighted mean RMSE and (green) pattern correlation for the horizontal distributions of (a–c) cloud forcing, (d) rainfall, and (e) precipitable water. Solid shows the global model bias and (dashed) just in the region 30S–30N, 50E–200E.

Overall, the insensitivities above support the hypothesis of *Pritchard and Bretherton* [2014] that restricting mesoscale dynamics in the 32–128 km horizontal scale regime may not fundamentally alter the basic physics that underpin SPCAM's MJO. Consistent with this view, lag-regression analysis in Figure 5 shows that for all tested configurations of SPCAM, to the east of the regression region at 10S, 10N 75E–100E, a convective OLR correlation streak moves through the regression zone at approximately the observed zonal phase speed, realistically flanked in longitude and time by oppositely signed low level wind anomalies. That is, the essence of an MJO signal exists in all configurations. Secondary modulations of the MJO are nonetheless evident due to reduced CRM extent. For instance, the zonal propagation of wind and convective anomalies through the eastern Indian Ocean equatorial regression zone is more coherent under Mini-CRM than in the standard model. This is a favorable refinement of the MJO signal, perhaps consistent with the shift to more on-equatorial OLR variance over the Indian Ocean noted in Figure 1, given the positioning of the reference regression region in this analysis. Distortions of the MJO include zonal wind zonal phase speed anomalies that are too fast in both Mini and Micro-CRM configurations. But, to first order, Mini-CRM has mostly preserved the existence and basic attributes of SPCAM's MJO signal from the perspective of OLR-wind lag regression analysis.

Robustness of SPCAM's MJO to reduced CRM extent has been further confirmed in trivariate empirical orthogonal function (EOF) analysis following the standard methodology of *Wheeler and Hendon* [2004] (not shown).

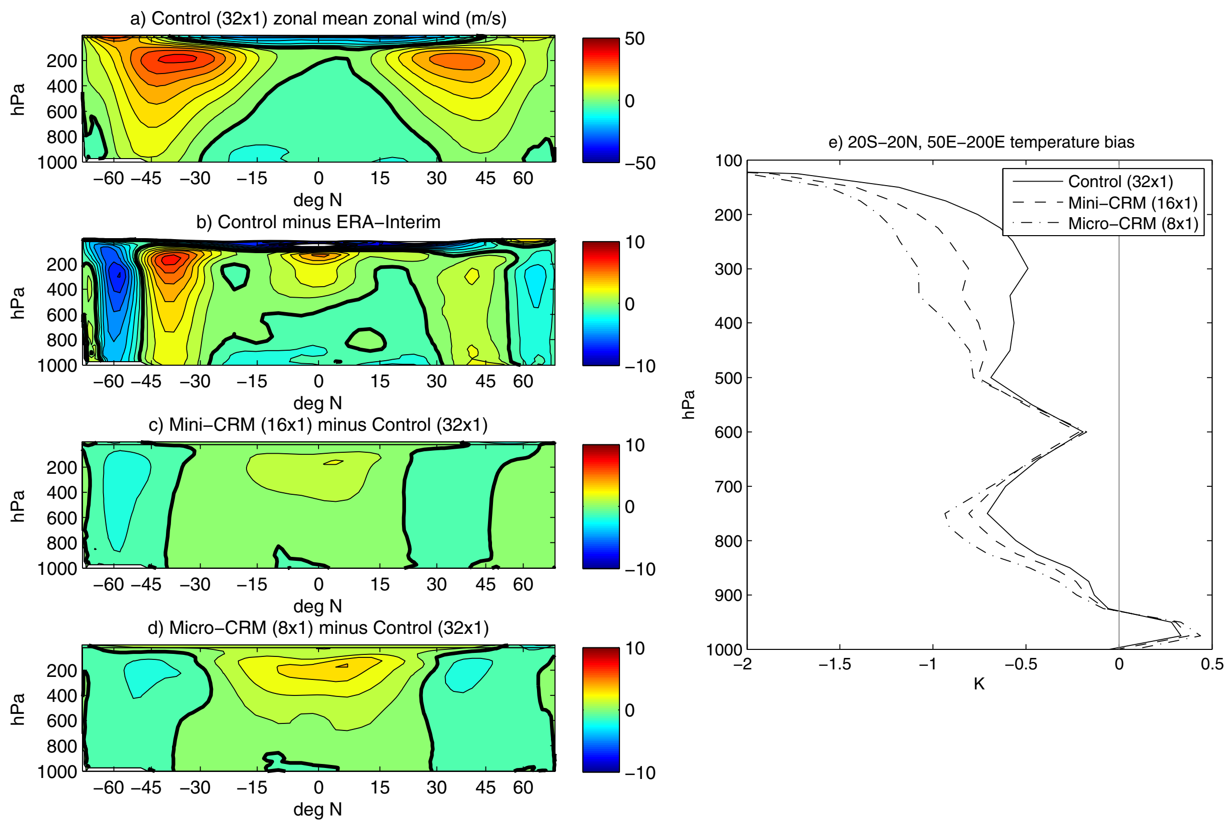

Figure 9. Annual zonal mean zonal wind climatology in (a) the control simulation (contour interval 5 m/s), (b) its bias relative to ERA-Interim reanalysis (contour interval 1 m/s), and (c and d) the additional anomalous zonal mean zonal wind in each test simulation (contour interval 1 m/s). Figure 8e shows the mean temperature bias profiles in the tropical Indo-Pacific region for each simulation.

In summary, eliminating the largest scales of mesoscale dynamics by reducing CRM extent produces a statistical composite MJO signature with spatial scale, zonal phase speed, and intrinsic wind-convection anomaly structure that are all remarkably similar to the standard SPCAM's MJO. Secondary changes to the MJO include favorably enhanced equatorial convective activity over the Indian Ocean, unfavorable wind anomaly zonal phase speedup, and favorable coherent convective propagation over the Maritime continent, as well as a favorable muting of local MJO variance there. Higher frequency tropical wave modes respond more than the MJO to reduced CRM extent, including a slight blurring of the MKW and MJO modes.

3.2. Mean State Response

The above analysis suggests that reducing CRM extent can achieve a key benefit of superparameterized simulations for MJO analysis with much less computational cost. However, aspects of the simulated mean state are more sensitive to the CRM extent, notwithstanding the discussion in *Khairoutdinov et al*. [2005].

Figure 6 compares the zonal mean cloud radiative forcing and precipitation in the control and test simulations against observational climatology. Particularly important features for deep convective disturbances and the MJO are the mean rainfall rate and associated longwave cloud forcing. Consistent with overall MJO insensitivity, these aspects of the zonal mean state are not strongly sensitive to Mini-CRM.

The mean shortwave cloud radiative forcing is more sensitive to reducing the CRM domain size. Figure 6a (blue lines) shows that the standard model already reflects far too much sunlight from tropical cloud systems, a well-known cloud optical bias in SPCAM [*Marchand and Ackerman*, 2010]. Mini-CRM and Micro-CRM tend to systematically amplify this bias even further. This does not appear to correspond to a geographical redistribution of rainfall because the region of enhanced shortwave cloud forcing (15S to 10N) coincides with both regions of decreased rainfall (e.g., 15S–5S) and increased rainfall (e.g., 0–10N; Figure 6b, red lines).

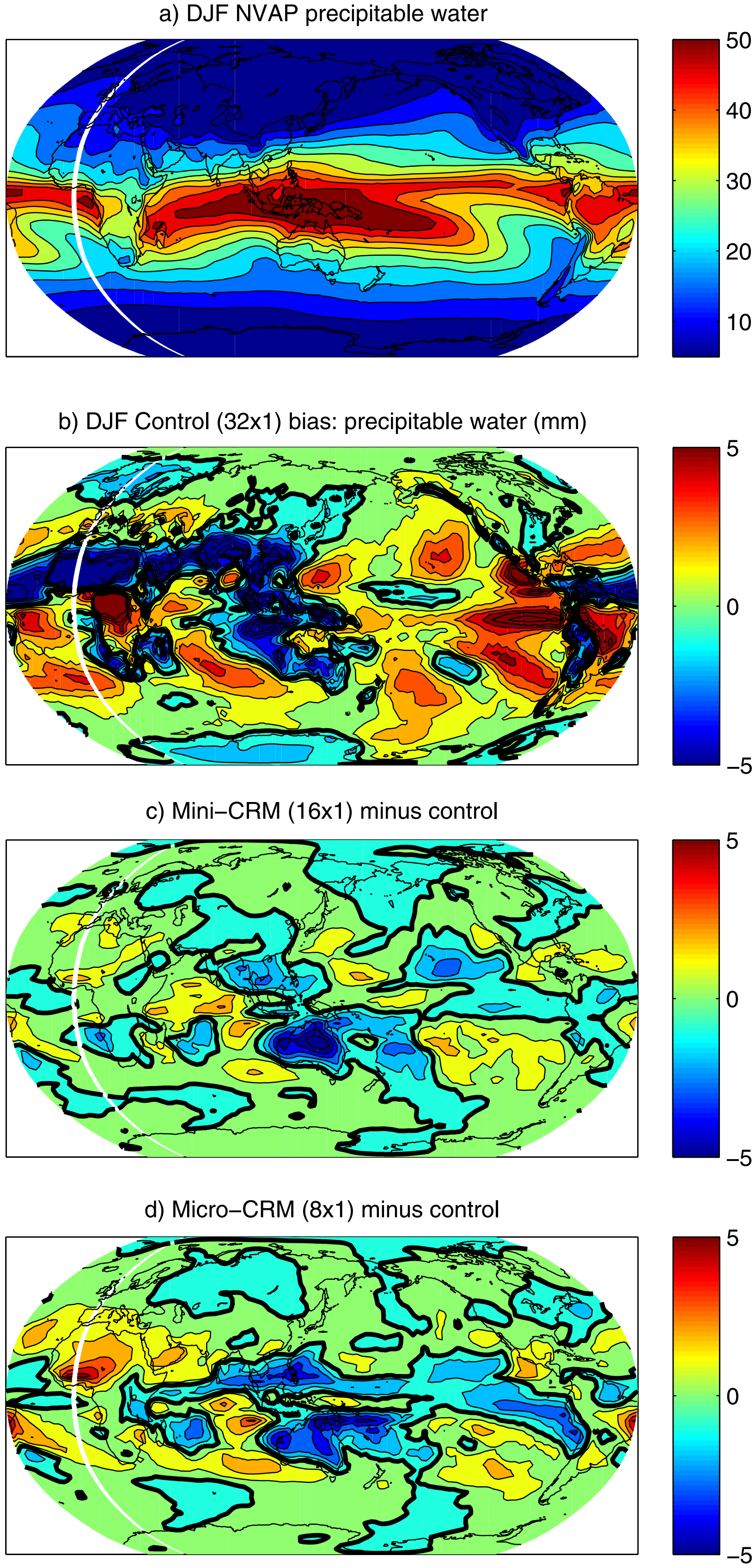

Figure 10. Annual mean precipitable water climatology in (a) the NVAP data product versus (b) the bias in the control version of SPCAM and (c and d) additional anomalous climatological vapor that results from reducing the CRM extent. Contour interval is 5 mm in Figure 9a and 1 mm in Figures 9b–9d.

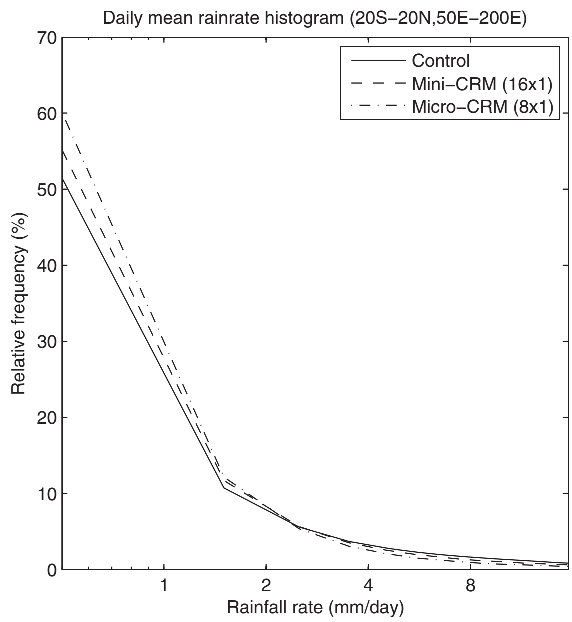

Figure 11. Relative frequency of daily mean precipitation rates throughout the 756 grid columns spanning 50E–200E and 20S–20N.

This seems to suggest a change in the underlying cloud population when using reduced CRM extent. We will return to this issue in the discussion section.

Figure 7 shows the geographic structure of the annual mean rainfall response to reducing the CRM extent. The control simulation produces too little tropical rainfall on the equator, and too much off the equator, particularly in the northern Indian Ocean, Bay of Bengal, and northwestern tropical Pacific. The latter bias has been attributed to an overactive monsoon in the boreal summer for this version of SPCAM and has been called the "Great Red Spot" [*Khairoutdinov et al*., 2005; *Luo and Stephens*, 2006]. Reducing the CRM domain extent does not affect the Great Red Spot but does tend to concentrate more rainfall on the equator and dry the SPCZ and north Indian Ocean, which are qualitatively favorable sensitivities.

Figure 8 summarizes the global (solid lines) and tropical Indo-Pacific (50E–200E, 30S–30N; dashed lines) biases in the annual mean horizontal pattern of mean rainfall, precipitable water, and cloud optical properties in all simulations. Reducing the CRM extent has little systematic extent on the model mean state biases in the longwave cloud radiative effect (CRE) and column water vapor and improves the tropical precipitation as noted above. However, there is a clear degradation of the shortwave CRE, as already suggested by the zonal mean biases.

Figures 9a–9d show the effect of reduced CRM extent on the general circulation. There is a slight enhancement of the baseline model's overly vigorous superrotation in the upper troposphere. But in general, all the model versions have a similar bias pattern relative to the ERA-Interim reanalysis. From the moisture mode view of the MJO, an especially important feature of the basic state flow is the low-level zonal wind, which is insensitive to CRM domain reduction. Figure 9e shows, however, that there is a slight amplification of the upper-tropospheric cold bias for reduced CRM domains. We will return to this feature in the discussion section.

The magnitude and horizontal pattern of basic state precipitable water is also important to the MJO from the moisture mode view. Mean state vapor is a moist static energy (MSE) reservoir that can help maintain MJO amplitude, and horizontal gradients of basic state column vapor constrain the rate at which the MJO can propagate via "self-advection," or the advection of the moisture field [*Pritchard and Bretherton*, 2014]. Figure 10 shows that reducing CRM extent tends to dry the atmosphere over Australia, southeast Asia, and the southwestern as well as northwestern tropical Pacific ocean in the annual mean whereas it tends to moisten the atmosphere on the equator adjacent to the Maritime Continent. During DJF (not shown) regional moistening in the southeastern Indian Ocean acts to resist an unrealistically strong zonal gradient of basic moisture in the control model that may explain (via advective consequences) the more coherent and faster eastward MJO propagation in this region when using reduced CRM extent.

In summary, consistent with an insensitivity in the MJO itself, many critical aspects of the thermodynamic and dynamic basic state in SPCAM are also mostly insensitive to the use of Mini-CRM

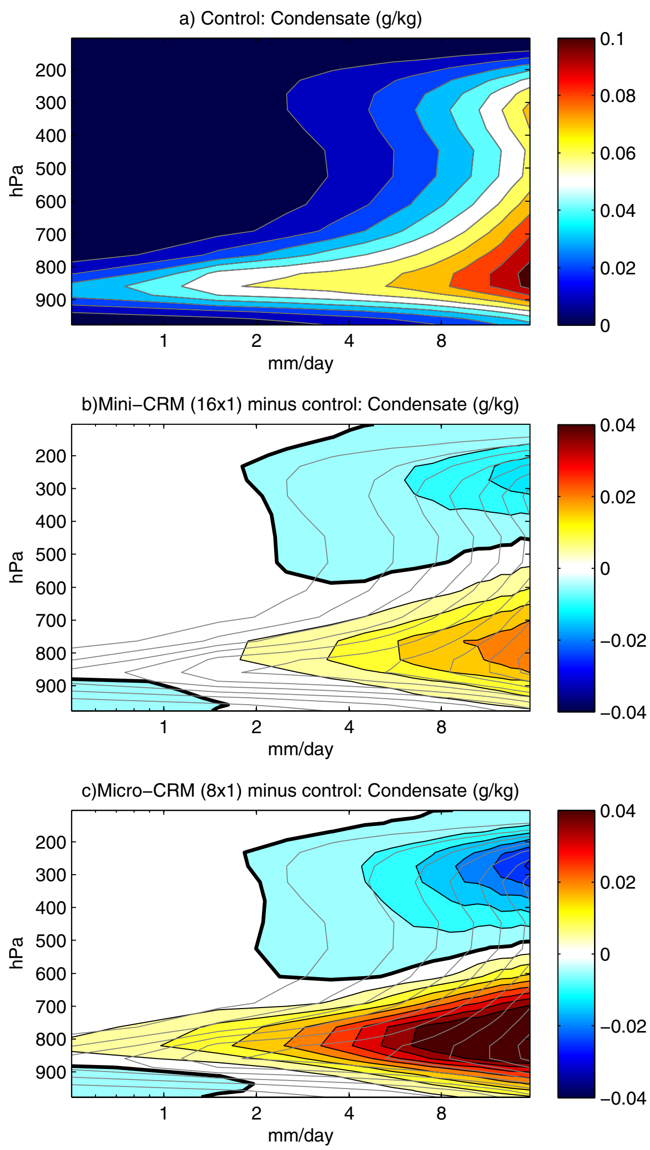

Figure 12. (a) Daily mean pressure and precipitation rate-composite of CRM-horizontal-mean total condensate (0.01 g/kg contour interval) in the control simulation accumulated for all seasons across 756 grid columns spanning 50E–200E and 20S–20N. (b and c) Difference in condensate (test minus control; 0.05 g/kg contour interval) in each pressure and precipitation rate bin.

(precipitation rate, horizontal pattern of low level zonal flow, longwave cloud forcing). Some secondary mean state sensitivities seem consistent with a moisture mode view of SPCAM's MJO such as phase speedup associated with reduced magnitude of the negative zonal precipitable water gradient in the southeastern tropical Indian Ocean.

4. Shortwave Cloud Forcing Biases and CRM Extent

We have noted a striking enhancement of shortwave cloud radiative forcing in the tropics resulting from reduced CRM extent.

This motivates the hypothesis that there is an interesting change in the nature of cloud vertical structure and hence cloud radiative feedbacks that tends to cause shortwave cloud effects to play an especially prominent role as CRM extent is reduced.

To gain some further insight into how reducing CRM extent affects the simulated cloud population, approximately seven hundred thousand daily mean model state profile snapshots were analyzed (756 model grid columns spanning the region 20S–20N, 50E–200E). To discriminate different convective regimes, CRM-domain-mean properties were binned by rain rate (1 mm bin spacing) throughout this region.

Figure 11 shows the rain rate histogram for each simulation in 20S–20N, 50E–200E. Reducing CRM extent shifts the distribution toward lower rain rate conditions throughout the region, consistent with the drier time mean atmospheric column in this region when using reduced CRM extent (Figure 9). The precipitation PDF shifts are subtle and seem unlikely to explain the SWCF response for reduced CRM extent.

Figure 12 shows the rain rate composited condensate composite profile, indicating that at all rain rates there is a *systematic increase* in the amount of condensate in the lower troposphere and a *systematic decrease* in the amount of condensate in the very highest portions of the upper troposphere when the CRM extent is reduced. A denser low, liquid cloud population is consistent with the finding of enhanced shortwave cloud forcing (Figure 5a).

The question naturally arises as to *why* liquid clouds in the tropics should enhance as a result of using small CRM domains. Figure 13 provides a clue in the geographic pattern of enhanced liquid water path, which

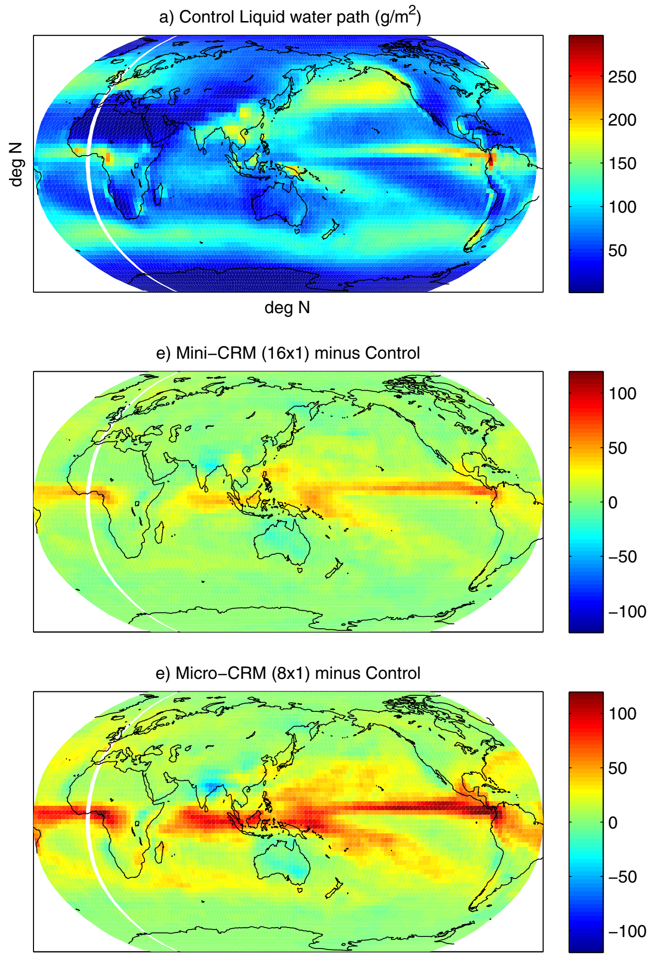

Figure 13. (a) Annual mean cloud liquid water path (CLWP; g/m^2) in the control simulation and (b and c) anomalous CLWP due to using Mini-CRM and Micro-CRM.

indicates that this effect occurs not only in the Warm Pool but in many tropical deep-convective regions, over both oceans and land.

We propose that a smaller CRM domain limits the efficiency of deep convective mixing by artificially restricting the room available for compensating subsidence. Figure 14 illustrates the proposed mechanism. In the standard large-domain CRM an isolated deep convective updraft only requires weak subsidence rates to balance it, since downward mass flux can be spread across a large compensating area. However, in a 2x (4x) smaller domain, the compensating subsidence rates for the same deep updraft would have to be 2x (4x) stronger inducing stronger subsidence warming that inhibits deep convection. Reduced vertical updraft mixing efficiency in turn predicts denser liquid clouds due to reduced ventilation of lower tropospheric moisture.

Consistent with the idea of reduced vertical mixing efficiency, Figure 9e has shown that reducing the CRM extent leads to a systematically cooler upper troposphere. This effect is nearly linear with respect to CRM domain size, as would be expected from the above view. Consistent with the idea that reduced deep mixing efficiency causes reduced ventilation, Figure 15 shows a systematic increase in lower tropospheric relative humidity that also scales with the CRM extent. A similar effect is seen for specific humidity (not shown).

Figures 16a and 16b confirm that consistent with the idea of domain-throttled deep convection there is a reduction of midtropospheric net upward mass flux in the CRMs stemming from weaker saturated updrafts. The relative humidity effect can thus be regarded as a response to having more cumulus detrain in the lower to mid troposphere and less in the upper troposphere.

It is natural to wonder how the idea of locally throttled deep convection fits into the broader energetic constraints of tropics-wide radiative convective equilibrium. Figures 16c and 16d show that there is remarkably little difference in the tropics-wide radiative cooling profile even when using small CRMs. Deep convection still has to make it up to the upper troposphere to balance radiative destabilization there despite the stronger subsidence resistance associated with small CRM domain sizes. Thus the upper level cooling under Micro-CRM can be viewed as a degree of freedom available to the environmental thermodynamic profile to help maintain RCE. That is, reducing thermal stratification compensates for the effects of stronger subsidence resistance. The drying aloft under Micro-CRM on regional scales suggests there is still a residual direct effect of throttled convection, which would tend to argue that environmental buffering can be "incomplete."

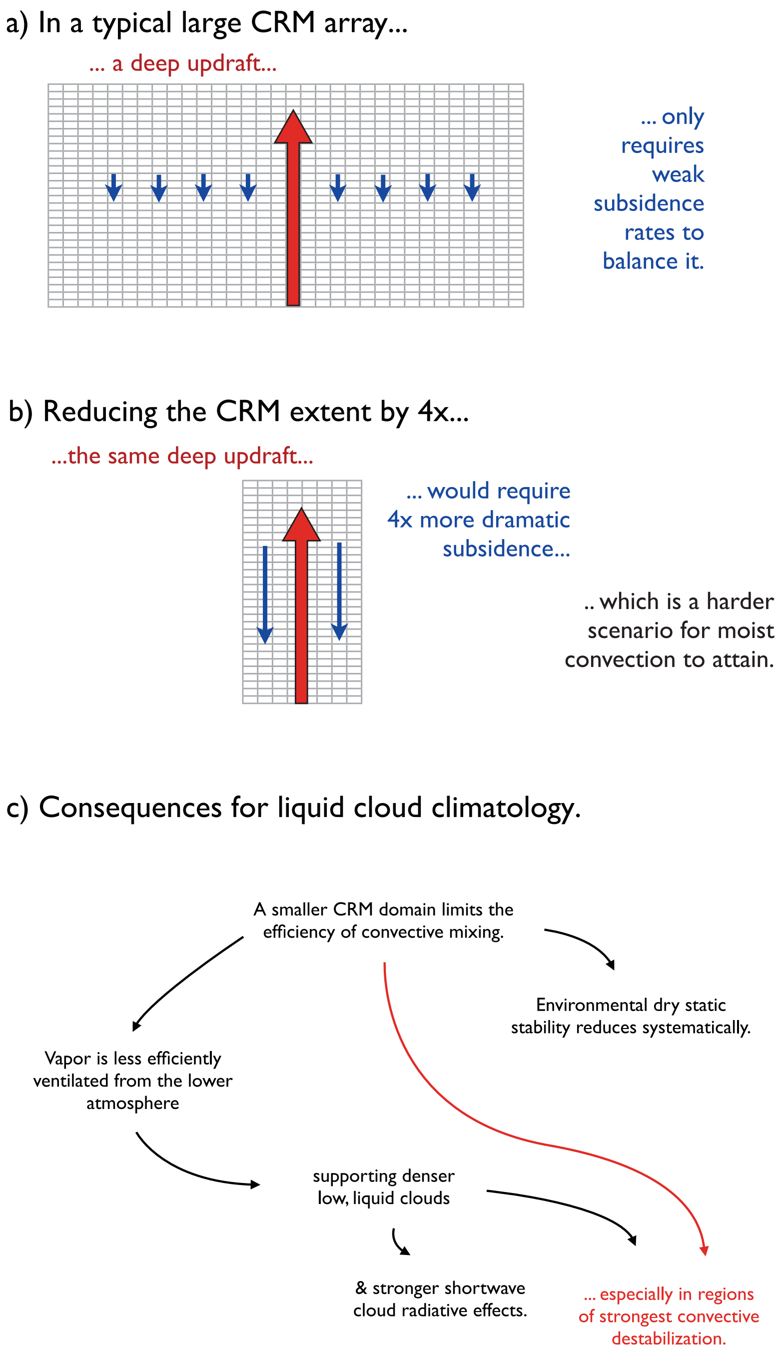

Figure 14. Proposed mechanism for why vertical convective mixing efficiency may decrease in tandem with CRM domain extent leading to more liquid clouds in deep convective zones.

This has implications for the intensity distribution of simulated deep convection. The insensitivity of the radiative cooling rate despite throttled midtropospheric mass fluxes implies that those deep cumulus that do reach the upper troposphere in the Micro-CRM configuration must have larger positive moist static energy (MSE) perturbations, so that enough MSE flux can be converged to balance the radiative cooling, even with less mass flux. That is, the cumulus spectrum under Micro-CRM must be broader, with a tail of more energetic clouds. This is consistent with the idea of a randomly excited and constantly destabilized system trying to overcome a stronger throttle—when it does overcome, it does so energetically.

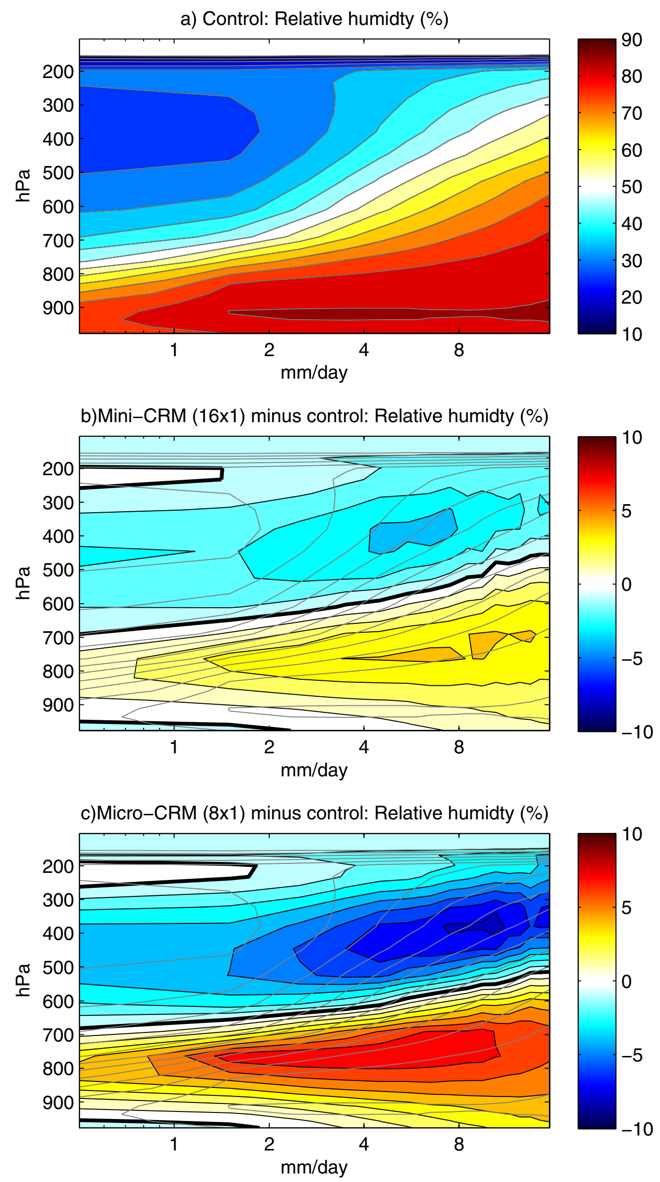

Figure 15. As in Figure 11 but for relative humidity using (a) 5% contour interval and (b and c) 1% contour interval. Results show systematic moistening of the lower troposphere as the CRM domain is reduced.

In summary, we view *more low-level liquid clouds as a consequence* of a relatively moister lower troposphere, in turn a consequence of reduced ventilation efficiency by deep updrafts, as limited by CRM domain size. This is consistent with the systematic effects of Mini and Micro-CRM on SPCAM's mean dry static stability, relative humidity, and low cloud concentration in regions of deep convection. But of course it cannot rule out other mechanisms that may be at play. For example, it is possible that a small CRM domain size reduces the frequency of deep convective triggering by limiting the number of candidate boundary layer thermals

It is interesting that the physics of MJO anomaly propagation are unaffected by this modulation of the background environment throughout the tropics. But a distortion of the fundamental physics of convective vertical mixing would caution against indiscriminate use of small-domain CRMs in superparameterized simulations.

5. Conclusions

The Madden-Julian Oscillation (MJO) in the uncoupled Superparameterized Community Atmosphere Model v.3.0 (SPCAM3.0) has been shown to be mostly insensitive to eliminating large scales of mesoscale dynamics through two and four-fold reductions in the horizontal extent of its embedded cloud resolving models (CRMs)—from 128 km, to 64 km, and 32 km.

The implication for MJO physics is that 32–128 km convective organization dynamics are not critical to the high quality MJO signal in SPCAM3.0. The results may support a moisture mode view of the MJO to the extent that subtle regional changes to MJO amplitude and phase speed are consistent with expectations from the thermodynamic mean state response to reduced CRM extent. For example, MJO amplification and phase speedup in the East Indian Ocean are associated with more background moisture and a relaxed negative background zonal moisture gradient there.

The practical implication for superparameterized simulation is that reducing CRM extent may be a viable strategy for 400% more computationally efficient analysis of MJO dynamics, as in *Pritchard and Bretherton* [2014]. However for studying cloud feedbacks on climate or other problems in which low cloud-radiation interaction plays a central role, reduced CRM extent will require more examination due

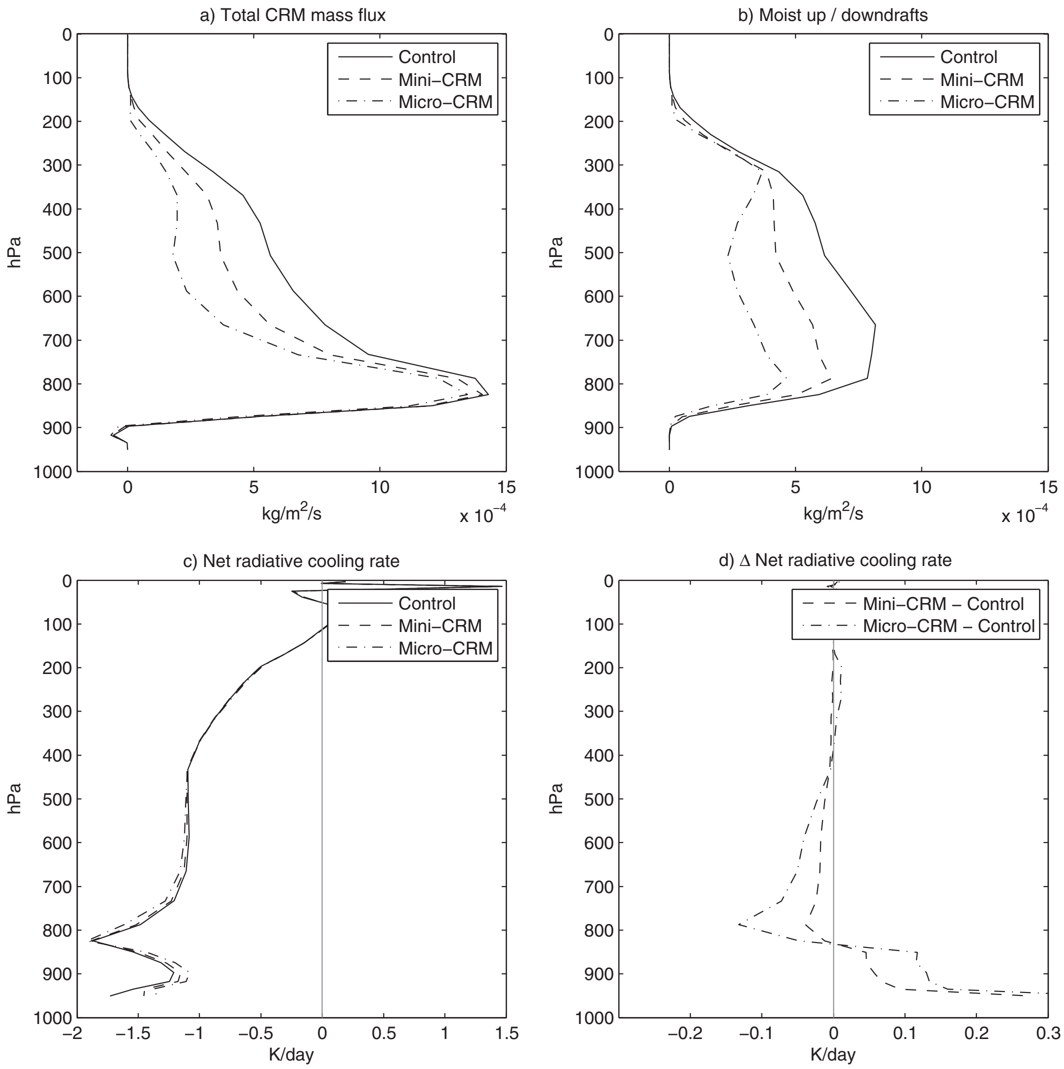

Figure 16. Annual, 15S–15N mean CRM-diagnosed (a) vertical mass flux and (b) its moist component in all simulations, as well as (c) the mean tropical radiative cooling rate including (d) the anomalies associated with reduced CRM extent.

to mean state responses promoting too much liquid condensate and associated shortwave cloud effects.

In particular, excessive mean state liquid condensate develops over convectively active regions as the CRM domain size is reduced. We believe that the efficiency of vertical mixing by deep updrafts is artificially limited by the CRM domain size in superparameterized simulations based on the room available for compensating subsidence. This can result in reduced ventilation supporting a moister and hence cloudier lower atmosphere. We have argued this mechanism is physically plausible and consistent with several model sensitivities. This bias may even slightly affect the mean state simulated with 32 column wide CRM domains, the current SP-CAM standard. However it seems likely that other representational issues such as the coarse horizontal and vertical grid are more important [e.g., *Marchand and Ackerman*, 2010]. Our argument suggests that the bias will scale inversely with the overall number of CRM grid columns rather than the physical domain size, as long as individual updrafts remain poorly resolved and therefore one or two grid points wide. It may be worth exploring whether the liquid and shortwave biases introduced by Micro-CRM can be compensated for by retuning unconstrained CRM microphysical parameters. In general, these considerations point to the need for more extensive study of the optimal CRM configuration for deploying superparameterization for climate change projection.

Acknowledgments
High performance computing resources for this work were provided courtesy of the Extreme Science and Engineering Discovery Environment (XSEDE), which is supported by NSF grant OCI-1053575, under allocations TG-ATM120034, TG-ATM120037, and TG-ATM130043. MP acknowledges the National Oceanographic and Atmospheric Administration's Climate and Global Change Postdoctoral Fellowship Program for funding preliminary results that led to this work. CB and CDM acknowledge additional support from the National Science Foundation (NSF) Center for Multiscale Modeling of Atmospheric Processes (CMMAP; grant ATM0425247). CDM acknowledges additional NSF support from grant AGS-1119999. We are grateful to Marat Khairoutdinov for developing and sharing SPCAM3.0 and to David Randall and Mark Branson for distributing it through CMMAP. All code and data needed to reproduce this analysis are archived by CMMAP and the corresponding author and can be made available to scientific researchers on request.

References

Benedict, J. J., and D. A. Randall (2009), Structure of the Madden-Julian Oscillation in the superparameterized CAM, *J. Atmos. Sci.*, *66*(11), 3277–3296.

Biello, J. A., and A. J. Majda (2005), A new multiscale model for the Madden–Julian oscillation., *J. Atmos. Sci.*, *62*(6), 1694–1721.

Grabowski, W. W. (2001), Coupling cloud processes with the large-scale dynamics using the cloud-resolving convection paramaterization (CRCP), *J. Atmos. Sci.*, *58*(9), 978–997.

Khairoutdinov, M., D. Randall, and C. DeMott (2005), Simulations of the atmospheric general circulation using a cloud-resolving model as a superparameterization of physical processes, *J. Atmos. Sci.*, *62*(7), 2136–2154.

Khairoutdinov, M., C. DeMott, and D. Randall (2008), Evaluation of the simulated interannual and subseasonal variability in an AMIP-style simulation using the CSU multi-scale modeling framework, *J. Clim.*, *21*(3), 413–431.

Khouider, B., and A. J. Majda (2006), A simple multicloud parameterization for convectively coupled tropical waves. Part I: Linear analysis, *J. Atmos. Sci.*, *63*(4), 1308–1323.

Kim, D., K. Sperber, and W. S. (2009), Application of MJO simulation diagnostics to climate models, *J. Clim.*, *22*(23), 6413–6436.

Luo, Z. Z., and G. L. Stephens (2006), An enhanced convection-wind-evaporation feedback in a superparameterization GCM (SP-GCM) depiction of the Asian summer monsoon, *Geophys. Res. Lett.*, *33*, L06707, doi:10.1029/2005GL025060.

Madden, R. A., and P. R. Julian (1972), Description of global-scale circulation cells in tropics with a 40–50 day period, *J. Atmos. Sci.*, *29*(6), 1109–1123.

Majda, A. J., and S. N. Stechmann (2009), The skeleton of tropical intraseasonal oscillations, *Proc. Natl. Acad. Sci. U. S. A.*, *106*(21), 8417–8422.

Marchand, R., and T. Ackerman (2010), An analysis of cloud cover in multiscale modeling framework global climate model simulations using 4 and 1 km horizontal grids, *J. Geophys. Res.*, *115*, D16207, doi:10.1029/2009JD013423.

Miyakawa, T., M. Satoh, H. Miura, H. Tomita, H. Yashiro, A. T. Noda, Y. Yamada, C. Kodama, M. Kimoto, and K. Yoneyama (2014), Madden-julian oscillation prediction skill of a new-generation global model, *Nat. Commun.*, *5*(3769), 1–6, doi:10.1038/ncomms4769.

Pritchard, M. S., and C. S. Bretherton (2014), Causal evidence that rotational moisture advection is critical to the superparameterized Madden-Julian Oscillation, *J. Atmos. Sci.*, *71*(2), 800–815.

Randall, D., M. Khairoutdinov, A. Arakawa, and W. Grabowski (2003), Breaking the cloud parameterization deadlock, *Bull. Am. Meteorol. Soc.*, *84*(11), 1547–1562.

Raymond, D. J., and Ž. Fuchs (2009), Moisture modes and the Madden-Julian oscillation, *J. Clim.*, *22*(11), 3031–3046.

Sobel, A., and E. Maloney (2012), An idealized semi-empirical framework for modeling the Madden-Julian Oscillation, *J. Atmos. Sci.*, *69*, 1691–1703.

Sobel, A., and E. Maloney (2013), Moisture modes and the eastward propagation of the MJO, *J. Atmos. Sci.*, *70*, 187–192.

Thayer-Calder, K., and D. A. Randall (2009), The role of convective moistening in the Madden–Julian oscillation, *J. Atmos. Sci.*, *66*(11), 3297–3312.

Wheeler, M. C., and H. H. Hendon (2004), An all-season real-time multivariate MJO index: Development of an index for monitoring and prediction, *Mon. Weather Rev.*, *132*, 1917–1932.

